

Packing circles and spheres on surfaces

Alexander Schiftner*
Evolute, TU Wien

Mathias Höbinger†
TU Wien

Johannes Wallner‡
TU Graz

Helmut Pottmann§
KAUST, TU Wien

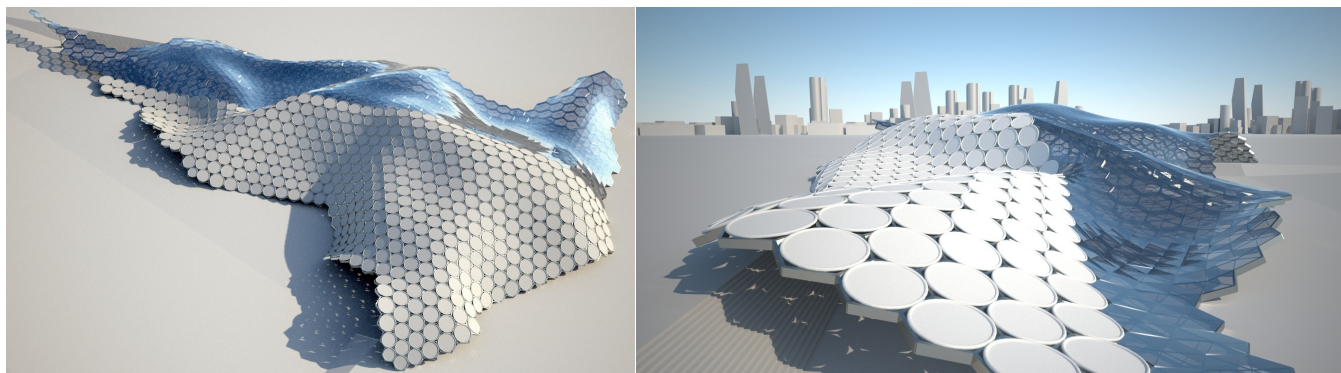


Figure 1: Resolving a freeform shape into circle-bearing hexagons. This is one of the many possible structures derived from a newly introduced type of triangle mesh, where the incircles of triangular faces form a packing. Such derived structures enjoy interesting properties relevant to both geometry and building construction.

Abstract

Inspired by freeform designs in architecture which involve circles and spheres, we introduce a new kind of triangle mesh whose faces’ incircles form a packing. As it turns out, such meshes have a rich geometry and allow us to cover surfaces with circle patterns, sphere packings, approximate circle packings, hexagonal meshes which carry a torsion-free support structure, hybrid tri-hex meshes, and others. We show how triangle meshes can be optimized so as to have the incircle packing property. We explain their relation to conformal geometry and implications on solvability of optimization. The examples we give confirm that this kind of meshes is a rich source of geometric structures relevant to architectural geometry.

CR Categories: I.3.5 [Computer Graphics]: Computational Geometry and Object Modeling—Geometric algorithms, languages, and systems; I.3.5 [Computer Graphics]: Computational Geometry and Object Modeling—Curve, surface, solid, and object representations

Keywords: computational differential geometry, architectural geometry, computational conformal geometry, freeform surface, circle packing, sphere packing, supporting structures.

*email: schiftner@evolute.at

†email: mathias.hoebinger@gmail.com

‡email: j.wallner@tugraz.at

§email: helmut.pottmann@kaust.edu.sa

1 Introduction

The motivation for the present paper comes from architectural projects which contain packing-like arrangements of circles on surfaces (see Fig. 2). In view of the beautiful geometry of circle packings in the plane and on the sphere (see [Stephenson 2005]), the question arises whether one can extend these results to surfaces. This is the main topic of our paper.

We present a new type of triangle meshes, where the incircles of the triangles form a packing, i.e., the incircles of two triangles with a common edge have the same contact point on that edge (Figures 3 and 4). These circle packing (CP) meshes exhibit an aesthetic balance of shape and size of their faces and thus are great candidates for applications in architecture. They are closely tied to sphere packings on surfaces and to various remarkable structures and patterns which are also of interest in art, architecture, and design. The focus of our work lies on computation and applications. Some of the underlying mathematics seems to be very difficult, so in some places we cannot offer proofs but only numerical evidence.



Figure 2: Arrangement of circles in freeform architecture. This image shows two different views of the Selfridges building, Birmingham, by Future Systems (right hand image courtesy P. Terjan).

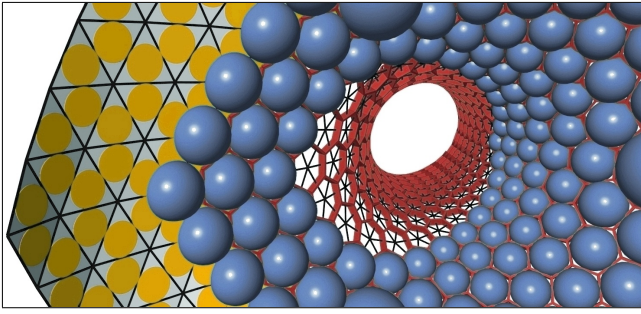


Figure 3: A CP mesh is a triangle mesh whose incircles (orange) form a packing. Then spheres (blue), which are centered at mesh vertices and are orthogonal to the incircles of neighboring triangles form a packing, too. Centers and axes of incircles define a hexagonal support structure with torsion-free nodes (red, see Section 3).

Related work. The present paper revolves around meshes which are endowed with additional circles or spheres. Relevant prior work therefore is research on circle packings, conformal mappings, and their geometry processing applications.

Complex analysis received a major impulse when W. Thurston proposed to study conformal mappings via circle packings. For instance, He and Schramm [1993] used this device to show the conformal equivalence of a quite general class of domains to ‘circle domains’ whose boundary is a possibly infinite collection of circles, thus proving an old conjecture of Koebe’s. Circle packings in general and especially their interpretation as discrete analytic functions / discrete conformal mappings are beautifully described in textbook form by K. Stephenson [2005]. For other circle patterns as discrete conformal mappings, see [Bobenko and Suris 2008].

Polyhedral surfaces endowed with circles are studied extensively [Gu and Yau 2008; Jin et al. 2008; Luo et al. 2008; Jin et al. 2009; Yang et al. 2009], in the context of topics like circle packing metrics and applications to discrete Ricci flow and optimized conformal parametrization. The CP meshes of the present paper are related in so far as they are meshes where the induced metric is a circle packing metric.

The Koebe meshes of Bobenko and Springborn [2004] have the CP property, and so do the isothermic meshes and discrete minimal surfaces of Bobenko et al. [2006]. In contrast to our work these are quad meshes with planar faces, describing isothermic surfaces (which means shape restrictions). All these constructions implicitly deal with conformal mappings, at least approximately so. An *exact* notion of conformal equivalence for triangle meshes appeared first in [Luo 2004]; it has recently been studied by [Springborn et al. 2008] for conformal flattening of surfaces whose topological type is a disk or sphere.

It recently turned out that both geometry and computational mathematics bear a great potential to advance the field of freeform architecture. The large number of unsolved problems and the increasing level of complexity in design are the source of the new research area *Architectural Geometry*, currently emerging at the border of differential geometry, computational mathematics and architectural design/engineering (see for example the monograph [Pottmann et al. 2007a] and the proceedings volume [Pottmann et al. 2008]). On a technical level, this paper deals with meshes with planar faces which approximate freeform shapes, as well as with meshes which allow for a *torsion-free support structure*. This means the layout of beams following the edges of a mesh, such that symmetry planes of beams intersect at node axes passing through

the vertices (for these node axes, see [Pottmann et al. 2007c] and Figures 10, 18).

Contributions. The notion of CP mesh (i.e., a triangle mesh whose incircles constitute a packing) generalizes – to the extent possible – the notion of planar circle packing to the surface case. Our main focus is optimization algorithms for the creation of CP meshes and to derive from them geometric structures relevant to architectural geometry. We do not attempt the difficult task of recreating the strong theory available in the planar case but nevertheless employ the conformal geometry of surfaces when explaining solvability of optimization. We believe that this research on meshes combined with circle packings, sphere packings, and torsion-free support structures is a substantial contribution to the processing of freeform geometry which goes beyond meshes and which is important for applications. In particular, our main results are:

- The geometry and optimization of CP meshes and their relation to conformal geometry.
- Hybrid meshes (tri-hex and others) derived from CP meshes which exhibit geometric properties relevant to architecture and building construction (such as planar faces, design flexibility, structural properties). Other kinds of derived meshes allow for a support structure with torsion-free nodes.
- Approximate circle packings and patterns on arbitrary freeform shapes.

2 Triangle meshes with an incircle packing

We start our study of CP meshes with some basic relations and elementary geometric properties. Consider a triangle with vertices $\mathbf{v}_1, \mathbf{v}_2, \mathbf{v}_3$, whose edges are tangent to the incircle at points $\mathbf{t}_{12}, \mathbf{t}_{23}, \mathbf{t}_{13}$ (see Fig. 4). The distances of these contact points to the vertices \mathbf{v}_i are denoted by r_i , e.g., $r_1 = \|\mathbf{v}_1 - \mathbf{t}_{12}\| = \|\mathbf{v}_1 - \mathbf{t}_{13}\|$. With the edge lengths $l_{ij} := \|\mathbf{v}_i - \mathbf{v}_j\|$, we have

$$l_{ij} = r_i + r_j, \quad 2r_i = l_{ij} + l_{ik} - l_{jk}. \quad (1)$$

Associated packing of spheres. Consider the star of triangles adjacent to the vertex \mathbf{v}_i . For a CP mesh, all contact points of incircles on edges through \mathbf{v}_i must lie at the same distance r_i from \mathbf{v}_i . Hence, r_i is a value associated with a vertex in the triangulation. Viewing r_i as radius of a sphere S_i with center \mathbf{v}_i , we arrive at a *sphere packing* (Fig. 3): Adjacent spheres S_i, S_j touch at \mathbf{t}_{ij} . Moreover, the sphere S_i is orthogonal to all incircles of triangles which share the vertex \mathbf{v}_i . Hence, we can say that the sphere packing is orthogonal to the packing of incircles.

Remark: This process of associating incircles and orthogonal spheres to a CP mesh can be reversed: it is clear that any collection of circles and orthogonal spheres yields a CP mesh, with one face per circle, and one vertex per sphere. When representing a CP mesh by this circle-sphere collection instead of its vertices, it becomes an object of Möbius geometry (see [Cecil 1992]): A Möbius

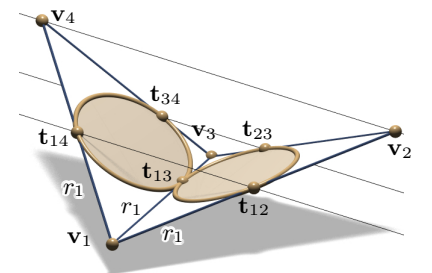


Figure 4: We introduce notation for a pair of adjacent triangles in a CP mesh: Vertices \mathbf{v}_j , points of tangency with incircles \mathbf{t}_{ij} , distances $r_i = \|\mathbf{v}_i - \mathbf{t}_{ij}\|$. Note that $\mathbf{t}_{14}, \mathbf{t}_{12}, \mathbf{t}_{34},$ and \mathbf{t}_{23} are co-planar.

transformation maps circles to circles, spheres to spheres, and preserves orthogonality. It therefore maps CP meshes to CP meshes.

Precise circle packings are rare. We employ the word *CP mesh*, since polyhedral metrics where edge lengths are defined by radii via (1) are called *circle packing metrics* (see e.g. [Gu and Yau 2008; Luo et al. 2008]). However, the incircle packing is not really a complete circle packing: for that, one would like to fill the gaps at vertices (Fig. 3), a topic to be addressed later on. It is important to note that there is no hope to get a precise circle packing which approximates an arbitrary shape. This is because circles touching each other lie on a common sphere and their axes of rotation are co-planar. Hence, the axes of a triple of pairwise tangent circles either pass through a common point, or are parallel. Continuing this argument, one sees that all circles of a precise packing which contains triples either lie in a common sphere or a common plane. Circle packings with *quadrilateral* combinatorics such as those of [Bobenko et al. 2006] do not fall under this limitation since they do not contain triples (but they cannot approximate general shapes, only isothermic surfaces).

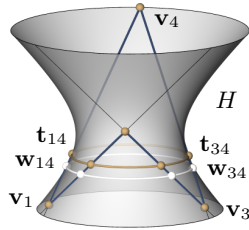
Two triangles with a common edge. In a CP mesh, we look at two triangles, $\mathbf{v}_1\mathbf{v}_2\mathbf{v}_3$ and $\mathbf{v}_1\mathbf{v}_3\mathbf{v}_4$ with a common edge $\mathbf{v}_1\mathbf{v}_3$ (Fig. 4). Expressing the edge lengths via (1), we immediately see that the sum of lengths of opposite edges in the quad $\mathbf{v}_1, \dots, \mathbf{v}_4$ is equal,

$$l_{12} + l_{34} = l_{23} + l_{14}. \quad (2)$$

Also the converse is true: If (2) holds, the two incircles meet in the common point \mathbf{t}_{13} . In order to see this, consider the triples of distances r_1, r_4, r_3 and r'_1, r'_2, r'_3 associated with triangles $\mathbf{v}_1\mathbf{v}_4\mathbf{v}_3$ and $\mathbf{v}_1\mathbf{v}_2\mathbf{v}_3$, respectively – not knowing yet that the two respective incircles meet in a common point, i.e., not knowing that in fact $r_1 = r'_1, r_3 = r'_3$. Now condition (2), which reads $r'_1 + r'_2 + r_3 + r_4 = r'_2 + r'_3 + r_1 + r_4$, together with the obvious equality $r_1 + r_3 = r'_1 + r'_3$ implies that $r_1 = r'_1$ and $r_3 = r'_3$.

In the plane, a quad which obeys (2) has an incircle, and also in space, condition (2) has interesting consequences: Consider the intersection point \mathbf{c} (may be at infinity) of the obviously coplanar lines $\mathbf{v}_2\mathbf{v}_4$ and $\mathbf{t}_{12}\mathbf{t}_{14}$. Projecting one incircle from center \mathbf{c} onto the plane of the other triangle results in the other incircle (since a conic is already defined by three tangents and the contact points on two of them). Hence, also the line $\mathbf{t}_{23}\mathbf{t}_{34}$ passes through \mathbf{c} and the contact points $\mathbf{t}_{12}, \mathbf{t}_{23}, \mathbf{t}_{34}, \mathbf{t}_{14}$ are coplanar (see Figures 4, 5); they also lie on the sphere containing the two incircles and thus these four points lie on a common circle c (their cross ratio is a Möbius invariant).

Remark: In Section 3 we make use of the following fact: The known distances r_1, r_2, \dots imply that the angle between the axis A of the circle c and each of the four edges of the quad is the same. Thus the lines carrying opposite edges can be transformed into each other by a rotation about A . It follows that all edges lie on a one-sheeted hyperboloid H whose axis is A . Observe further that new points \mathbf{w}_{ij} located on the edge $\mathbf{v}_i\mathbf{v}_j$ at constant distance from \mathbf{t}_{ij} lie on a common circle.



2.1 Optimization algorithm

In order to compute CP meshes that approximate a given freeform surface Φ , we formulate an optimization problem for the vertices of an initially given triangle mesh. The target functional is given by

$$F = \lambda_1 f_{cp} + \lambda_2 f_{prox} + \lambda_3 f_{prox}^{\partial}, \quad (3)$$

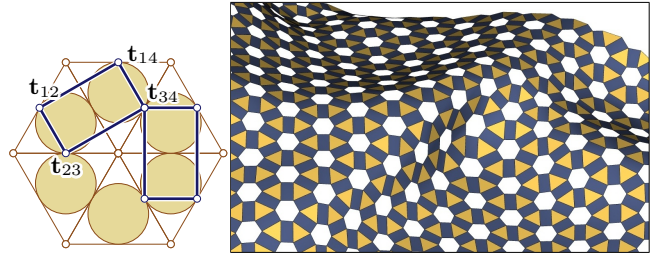


Figure 5: This pattern formed by triangles, planar (even circular) quads and non-planar hexagons is derived from a CP mesh by connecting appropriate contact points of incircles.

where f_{cp} measures the incircle packing property, f_{prox} measures proximity of the mesh to the reference surface, and f_{prox}^{∂} quantifies proximity of the mesh boundary to $\partial\Phi$. In view of (2) we let

$$f_{cp} = \sum_{\text{interior edges } \mathbf{v}_i\mathbf{v}_j} (l_{ik} + l_{jm} - l_{kj} - l_{im})^2, \quad (4)$$

where $\mathbf{v}_i\mathbf{v}_j\mathbf{v}_k$ and $\mathbf{v}_i\mathbf{v}_j\mathbf{v}_m$ are the faces adjacent to the edge $\mathbf{v}_i\mathbf{v}_j$. For an alternative target functional we use the radii r_i as additional variables and replace f_{cp} by

$$f_{bp} = \sum_{\text{edges } \mathbf{v}_i\mathbf{v}_j} (\|\mathbf{v}_i - \mathbf{v}_j\| - r_i - r_j)^2. \quad (5)$$

This allows us to prescribe certain sphere radii r_i . For the definition of the proximity terms in (3), we use the symbols π and $\tilde{\pi}$ for the closest point projections onto the surface Φ and its boundary $\partial\Phi$, respectively. Further, $\tau_{\mathbf{x}}$ denotes Φ 's tangent plane in the point \mathbf{x} , and $T_{\mathbf{x}}$ denotes the tangent of the boundary curve $\partial\Phi$. We let

$$f_{prox} = \sum_{\text{vertices } \mathbf{v}_i} \text{dist}(\mathbf{v}_i, \tau_{\pi(\mathbf{v}_i)})^2, \quad f_{prox}^{\partial} = \sum_{\text{bdry vertices } \mathbf{v}_i} \text{dist}(\mathbf{v}_i, T_{\tilde{\pi}(\mathbf{v}_i)})^2.$$

Numerics and convergence. The optimization problem “ $F \rightarrow \min$ ” is a nonlinear least squares problem for the vertex locations of the mesh under consideration. The reference surface Φ enters optimization via the closest point projections π and $\tilde{\pi}$. So for purposes of optimization we may assume that Φ is given by these two projections and we do not care about how Φ is actually represented.

We use a damped Gauss-Newton method to compute minimizers. The required first order derivatives are computed exactly. The fact that all single contributions to F are local leads to the important property that the linear system to be solved in each optimization step is sparse. We employed CHOLMOD for sparse Cholesky factorization [Chen et al. 2008], which we found to be faster than TAUCS [Toledo 2003]. Comparing results for the functionals f_{cp} and f_{bp} , only minor differences in the minimizers could be noticed. Typically f_{bp} leads to faster convergence (by about 10%) than f_{cp} despite the fact that the number of variables is bigger by one third.

In case Φ is a topological disk or sphere, we initialize optimization by choosing an arbitrary triangle mesh that already approximates Φ reasonably well. We experienced convergence towards a precise CP mesh in all such cases. Figures 6, 7, 8 show results for different mesh connectivities approximating the same reference surface. Timings are for a 2.4GHz PC, and we use the target functional of (3) with $\lambda_1 = \lambda_2 = \lambda_3 = 1$. The quality of the circle packing is measured by the descriptor

$$\delta_{bp} = \max_{\text{edges } \mathbf{v}_i\mathbf{v}_j} \left| 1 - \frac{r_i + r_j}{\|\mathbf{v}_i - \mathbf{v}_j\|} \right|,$$

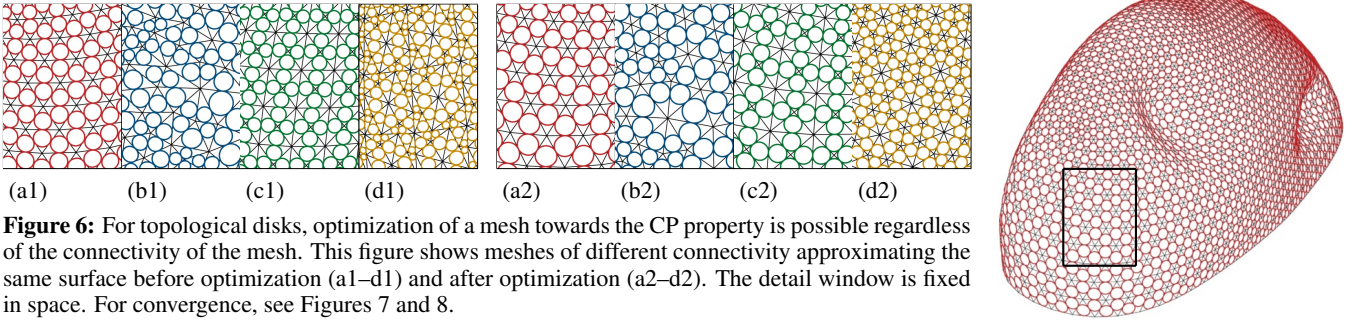


Figure 6: For topological disks, optimization of a mesh towards the CP property is possible regardless of the connectivity of the mesh. This figure shows meshes of different connectivity approximating the same surface before optimization (a1–d1) and after optimization (a2–d2). The detail window is fixed in space. For convergence, see Figures 7 and 8.

Model	n	# Iter.	sec	δ_{bp}	δ_{prox}	δ_{prox}^∂
(a) —	5612	8	2.17	5.8e-15	3.3e-15	7.3e-30
(b) —	6492	7	2.02	7.9e-15	5.5e-15	4.3e-29
(c) —	9860	9	4.04	1.7e-14	3.0e-15	4.4e-30
(d) —	15856	8	6.29	2.3e-15	3.2e-15	1.3e-29

Figure 7: Optimizing the meshes of Fig. 6 which approximate the same reference surface. We show the number n of variables, the number of iterations, computation time, and the quality measures δ_{bp} , δ_{prox} , δ_{prox}^∂ (see also Fig. 8). Bounding box diameter equals 70.

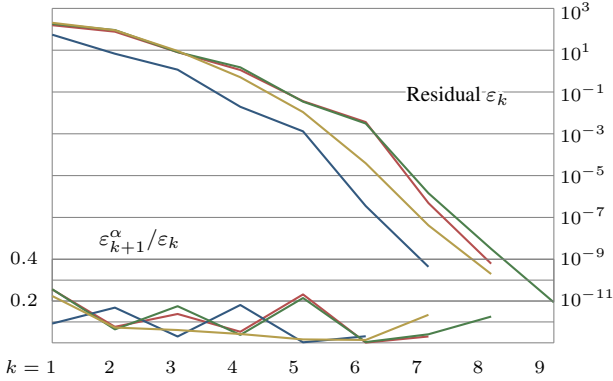


Figure 8: Convergence behaviour of optimization for the meshes of Figures 6, 7, where precise CP meshes exist. *Above:* Behaviour of the residual ε_k during optimization. We use an ℓ^2 distance of the mesh at iteration step $\#k$ to the final mesh (ε_k^2 being the sum of squares of distances of corresponding vertices). *Below:* Convergence is superlinear, since $\varepsilon_{k+1}^\alpha / \varepsilon_k$ is bounded for $\alpha = 0.85$.

and proximity to Φ and $\partial\Phi$ is measured by

$$\delta_{prox} = \max_{\text{vertices } \mathbf{v}_i} \text{dist}(\mathbf{v}_i, \tau_{\pi(\mathbf{v}_i)}), \quad \delta_{prox}^\partial = \max_{\text{bdry vertices } \mathbf{v}_i} \text{dist}(\mathbf{v}_i, T_{\tilde{\pi}(\mathbf{v}_i)}).$$

Convergence is very fast. Pure Gauss-Newton minimization in case of zero residual should converge quadratically; our numerical experiments still exhibit superlinear convergence (see Fig. 8).

2.2 Solvability of the optimization problem

As an introduction, we first discuss conformal mappings in the plane. Two planar circle packings with the same combinatorics, covering domains D, D' , define a discrete conformal mapping from D to D' . As such mappings approximate continuous conformal ones, this definition is meaningful [Stephenson 2005]. Another interpretation of two domains D, D' , conformally equivalent in the

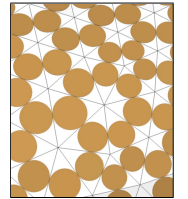
previous sense, is the following: The combinatorics of the circle packing store the discrete *conformal equivalence class* of the domain it covers, and D, D' are particular shapes contained in this class.

For many topological types of domain it is known that among the conformally equivalent ones there is a *canonical shape* whose boundary consists of circles (see He and Schramm [1993] who use circle packings in their proof). A similar relation between discrete and continuous conformal equivalence is true for the Schramm circle patterns and s-isothermic meshes of [Bobenko et al. 2006], which actually are quadrilateral CP meshes.

In view of their definition and Möbius invariance, our CP meshes are analogous to the constructions above, and we employ this analogy to the known cases to predict when our optimization succeeds. The argument is as follows: If a CP mesh approximates a given surface Φ , then the conformal equivalence class of Φ is the one of the mesh. If we start optimization with a mesh (not yet CP), its combinatorics already determine the conformal class which might or might not contain the shape of Φ . Obviously optimization can succeed only if this happens to be the case.

(i) Assume that Φ is a closed surface of genus g . The genus 0 surfaces (topological spheres) constitute a single conformal class [Stephenson 2005], and a mesh approximating Φ is in it, because it also has genus 0. Optimization therefore can succeed, as indeed confirmed by numerical experiments. For $g > 0$, there is a continuum of conformal classes (see [Luo et al. 2008]), and the initial mesh is unlikely to be conformally equivalent to Φ . Optimization usually fails unless the initial mesh is adapted to Φ , e.g. as follows:

Using the idea of [Alliez et al. 2005], we use a centroidal Voronoi diagram (computed by iterative Lloyd relaxation, (see [Liu et al. 2009])) to obtain an isotropic mesh which covers Φ , and which is used to initialize optimization (see Fig. 9a). This kind of optimization, however, leads to a rather random placement of singularities, which may be undesirable.



(ii) Assume that Φ is homeomorphic to a planar domain with b boundaries. All topological disks (case $b = 1$) are conformally equivalent, so optimization succeeds like for spheres. A topological cylinder ($b = 2$) is conformally equivalent to an annulus $r^2 < x^2 + y^2 < 1$ in the plane, and its conformal class is characterized by the value r . Optimization succeeds only if the r values associated with the mesh combinatorics and with Φ coincide. Fortunately we can easily change Φ 's r value by downweighting f_{prox}^∂ and allowing the mesh boundary to deviate from $\partial\Phi$: the mesh then covers a modified surface Φ^* . Numerical experiments confirm that optimization succeeds, but to a lesser extent. If $b > 2$ the canonical shape is an annulus with further circular holes whose position and size characterize the conformal class. Optimization is much harder.



Figure 9: CP mesh optimization for surfaces of higher topological complexity. (a) *Closed surfaces:* CP mesh with torus topology initialized from a centroidal Voronoi diagram. The associated sphere packing is shown in yellow, with spheres at irregular vertices (valence $\neq 6$) highlighted in red. (b) *Surfaces with boundary:* The triangle mesh of the Great Court roof, British Museum, London, by Chris Williams. (c) This mesh has been taken as both reference surface and initial mesh for CP optimization, with f_{prox}^{∂} applying only to the outer boundary. Figures describing optimization are similar to those of Fig. 7. Obviously the reference surface does not quite belong to the conformal class of surfaces defined by the mesh combinatorics.

(iii) If Φ is a surface of genus g with b boundaries ($g, b > 0$), then describing the canonical shape of a conformal class, such as done e.g. by [He and Schramm 1993, Th. 0.2], requires the concept of a Riemann surface. Basically the finitely many degrees of freedom which describe the shape of such a surface, together with the position and size of circular holes, are characteristic of a conformal class. The situation is therefore similar to (ii), and we cannot hope that optimization succeeds unless the initial mesh is already adapted to Φ .

Relation to conformal parametrization. In view of the above it seems natural to initialize optimization via some conformal parametrization. For the applications we have in mind, however, the inevitable distortions of such mappings are an obstacle. In fact, it is much more convenient to compute directly in space.

3 Derived structures

Hexagonal and other dual structures. R. Buckminster Fuller, Frei Otto, L. Spuybroek, and others have been fascinated by the shapes and structural efficiency of the silicious micro-skeletons of *radiolaria*, whose shapes are often based on hexagonal meshes [Bach 1990; Spuybroek 2004]. Aesthetically balanced versions of those can easily be derived as a dual of CP meshes with vertices of valence 6: We just have to connect the centers of tangent incircles. Fig. 3 shows an example of this. *Quad-octagon structures* can be made in a similar way, by starting with a CP mesh of quad-dominant connectivity (see Fig. 10).

Torsion free beam layout. If we physically realize a mesh and let beams follow its edges, the intersection of beams near vertices is an important issue. It is desirable that symmetry planes of beams nicely intersect in a common *node axis* which passes through a vertex. Such beams are called a support structure with torsion-free nodes (see [Pottmann et al. 2007b; Pottmann et al. 2007c]). With our dual meshes, this is easy to accomplish: node axes are axes of incircles (because neighbouring incircle axes lie in a common plane, orthogonal to the common tangent of those incircles).

Remark: Note that the support structure achieved in this way is contained in the power diagram of the sphere packing associated with a CP mesh (for the notion of power diagram, which generalizes the Voronoi diagram, see [Aurenhammer 1987]). Note also that

[Pottmann et al. 2007c] does not apply to our situation, since it deals with planar faces only.

Filling hexagons. The nonplanar hexagonal faces which occur in this kind of construction may be filled in various ways. One way is by triangles (not used in this paper except for the ‘glass part’ of the structure in Fig. 1). Another way is shown by Fig. 11: By inserting a new vertex for each hexagonal face we split that face into three quads. Subsequent optimization allows vertices to move (but still draws them near incircle axes) and penalizes nonplanarity of the newly introduced quads. This results in a honeycomb structure which is obviously not smooth. For interior designs (acoustic damping) this might even be desirable.

Tri-hex meshes. The incircle contact points around a valence 6 vertex in a CP mesh define a hexagon, and holes between these hexagons are triangular. It turns out that such a mesh can be optimized for planarity of its faces and leads to very interesting structures (see Fig. 16 below). Without writing down the explicit formulas we mention that optimization minimizes a target functional which penalizes (i) distances of diagonals in hexagons, i.e., nonplanarity; (ii) deviation of vertices from a circumscribed sphere and deviation of the face’s center of mass from the sphere center, i.e., irregularity; (iii) deviation of vertices from the original incircle contact points. A result is shown in Fig. 12.

Approximate circle packings and patterns. Even if precise circle packings (formed by triples) do not exist on an arbitrary surface Φ , there are various ways to compute practically useful approximate versions of circle packings once we have found a CP mesh for Φ . For example, we extend the incircle packing of a CP mesh

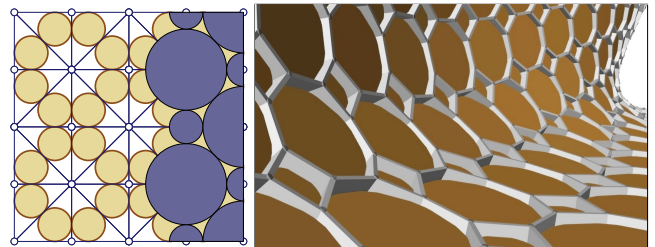


Figure 10: *Left:* A CP mesh with vertices of valences 4 and 8, with associated sphere packing. *Right:* Derived quad-octagon support structure with torsion-free nodes.

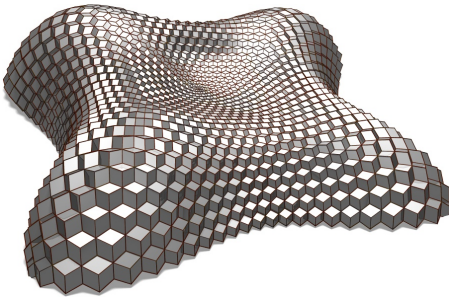


Figure 11: Filling hexagons with quads creates a honeycomb with torsion-free support structure. The underlying CP mesh is the same as for Fig. 12.



Figure 12: Tri-hex structure derived from a CP mesh whose hexagons are almost planar, and as regular as possible. See also Fig. 16 for a supporting framework.

by fitting a single circle into each vertex gap, which involves a separate least squares optimization with six variables for each circle (see Fig. 13a). Alternatively, a circle packing can be derived from the sphere packing by fitting a circle through the contact points of each sphere with its neighbours (see Fig. 13b).

The second method yields circles which together with the original incircles constitute an approximate Schramm’s circle pattern (see [Bobenko et al. 2006]) which covers Φ (see Fig. 15 in the discussion section below). It typically yields smaller gaps between adjacent circles than the first method, as the error is being distributed more evenly among the circles, which especially applies to mesh areas with non-uniform incircle sizes.

We should remark that a dramatic reduction of computation time at the cost of precision can be achieved by simply intersecting each sphere with a regression plane defined by its contact points. The quality of these approximations depends heavily on the Gaussian curvature of the underlying surface: areas with negative curvature

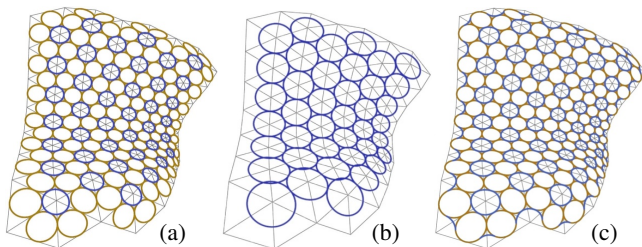


Figure 13: Approximate circle packings from CP meshes. (a) Circles (blue) approximately filling vertex gaps and being tangent to incircles. (b) Circles trying to connect the tangency points of incircles. (c) Arc splines (blue) exactly tangent to incircles.

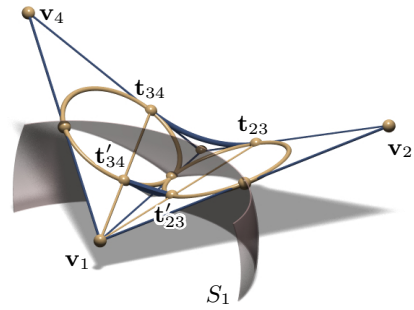


Figure 14: We use inversion to connect two adjacent incircles by a circular arc $t_{23}t_{34}$. This leads to a filling of holes with arc splines.

are problematic, which is consistent with the observation that precise circle packings exist only on spheres and planes.

Packings of circles and arc splines. The vertex gaps of the incircle packing can be nicely filled with arc splines as follows. We look at a triangle pair as in Figures 4 and 14. Obviously, there is a circular arc from t_{23} to t_{34} which smoothly connects the two incircles. Inversion with respect to the sphere S_1 (having radius r_1 and center at v_1) maps each incircle to itself (since it is orthogonal to S_1) and maps the arc $t_{23}t_{34}$ to a circular arc $t'_{23}t'_{34}$ which provides a smooth connection of the two incircles near v_1 . The contact point t'_{23} is collinear with t_{23} and v_1 , and analogously for t'_{34} . In this way we obtain a smooth curve formed by circular arcs which fills each vertex gap. By construction, the resulting packing is an object of Möbius geometry (see Fig. 13c).

Almost-rhombic quad meshes and sphere packings. We would like to give the name *almost-rhombic* to a mesh where each quad obeys (2), i.e., the sums of lengths of opposite edges are equal. It is interesting that we can find spheres centered in the vertices which form a packing with quad combinatorics, together with a system of circles which connect the contact points along face perimeters. If the angles of intersection between circles and spheres were 90 degrees, the mesh would be a discrete s-isothermic surface [Bobenko et al. 2006]. Since such surfaces have shape restrictions our circle/sphere pattern is the best one can hope for in general.

For a proof of these properties, consider a quadrilateral $v_1v_2v_3v_4$ in space which obeys (2). It can be decomposed in to a CP pair of triangles according to Figures 4 and 14. Using the notation of

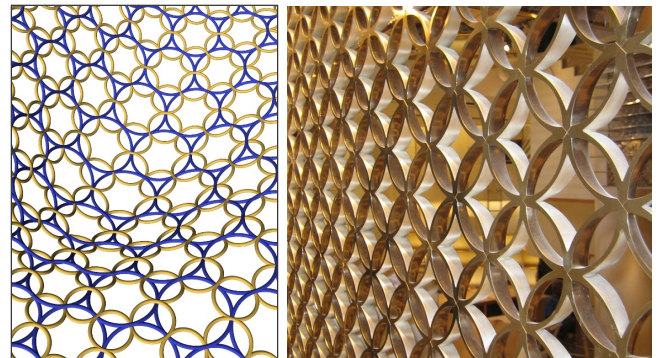


Figure 15: Left: Freeform circle pattern consisting of the incircles of a CP mesh and approximately orthogonal circles (blue) which covers a freeform surface. Right: A planar circle pattern design used for a screen in the Louis Vuitton Store, Paris.

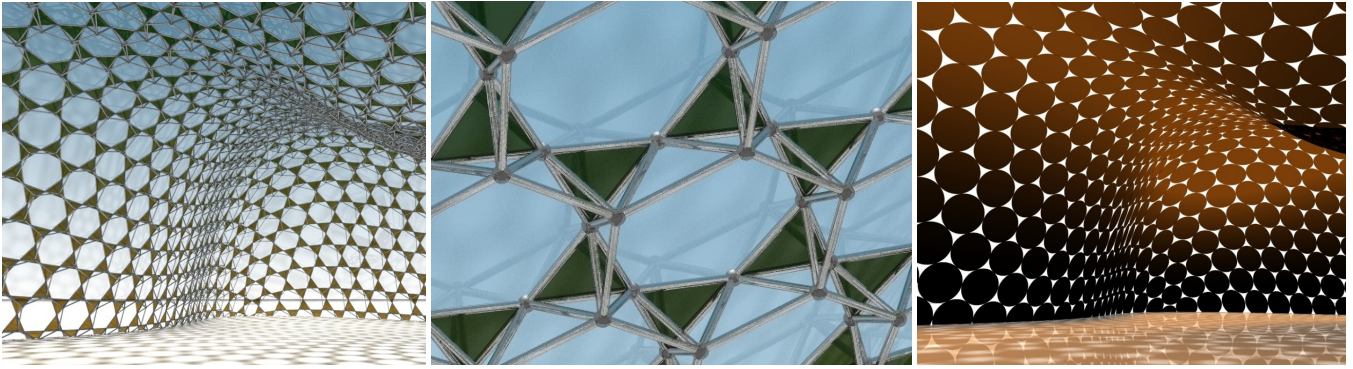


Figure 16: Structures derived from a CP mesh. *Left:* Interior view of the hybrid tri-hex mesh of Fig. 12 which is derived from a CP mesh. *Center:* Closeup of a supporting framework which makes use of the triangles present in the mesh. This solution has favorable statics and has been inspired by the Eden project, Bodelva, Cornwall, by N. Grimshaw (which however represents spherical shapes and where a different layer in the framework plays the role of the roof). *Right:* An approximate circle packing following the same shape, where optimization has been initialized not from the original CP mesh, but this time from the tri-hex mesh.

these figures, we have the spheres S_1, \dots, S_4 with radii r_1, \dots, r_4 and contact points t_{ij} . Obviously increasing the radii of spheres S_1, S_3 and decreasing the radii of S_2, S_4 by the same amount Δr (or vice versa) leads to spheres which still touch each other. The points of contact, now called w_{ij} , have moved by Δr along the edges. We have already seen that they are co-circular. It is now clear how a sphere packing can be constructed: Choose one sphere arbitrarily, all the remaining ones are uniquely determined by the contact condition.

The contact points w_{ij} determine a quad mesh where one half of the faces are planar (indeed, circular). Fig. 17 shows an example of this. Approximation of a given surface Φ by an almost-rhombic mesh can be done by optimization, with the target functionals f_{bp} and f_{prox} , and an additional beauty term which penalizes big differences in radii of adjacent spheres.

4 Discussion and examples

A main point in our treatment of CP meshes is the wealth of meshes and structures derived from them. In particular, the hybrid meshes with planar faces can approximate arbitrary shapes in a way very different from the pure quad or pure hex mesh case, where planar faces entail a rigid dependence of the mesh on surface curvatures (see [Liu et al. 2006] and [Pottmann et al. 2007c]).

It is also remarkable that such meshes have favorable structural

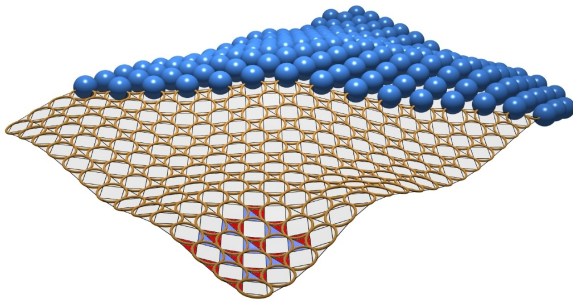


Figure 17: Sphere packing (blue) with circle pattern derived from an almost-rhombic mesh (not shown). The contact points of spheres are the vertices of a hybrid tri-quad mesh, whose quads are circular. In the lower part of the figure, the triangular faces are marked.

properties (which basically comes from the triangles contained in them). An example is given by Fig. 16, where a freeform shape is approximated first by a CP mesh and subsequently by a derived tri-hex mesh. The latter is supported by a framework which utilizes the triangles contained in the mesh in an essential way (Fig. 16, center). With such a structure we even succeed to place planar and convex (nearly-regular) hexagons in negatively curved areas of a surface. A pure hex mesh would require non-convex faces there, if faces are required to be planar. We should mention that due to space limitations we did not fully discuss all interesting geometric properties of hybrid meshes (like the existence of parallel meshes and torsion-free support structures). The ornamental character of various derived structures makes them appealing for interior design (see Fig. 16, right, Fig. 15, and Fig. 18).

Limitations. The main limitation in the process of approximating an arbitrary shape by a CP mesh lies in the fact that optimization succeeds for topological spheres and disks, to a lesser extent for topological cylinders, and usually does not succeed for surfaces of higher topological complexity. The reasons for that are discussed at length in Section 2.2. The way around which is proposed here (centroidal Voronoi diagrams) leads to irregular meshes possibly unsuitable for the purpose in mind. However, recall that the main application of the algorithms and constructions described in the present paper is geometric structures for architecture in a broad sense, where the disk and cylinder topologies are the most frequent.

Conclusion and future research. We have introduced and discussed ‘circle packing’ meshes with regard to both their geometry and their approximation properties, and we showed applications and structures derived from such meshes. It turns out that CP meshes constitute a new link between architectural freeform design and computational conformal geometry.

Many interesting questions in this area are still unexplored. One direction of research is the Möbius geometry of CP meshes (e.g. the meaning of the cross ratios which occur in them). Another one is their relation to conformal geometry, both algorithmically and theoretically: The present paper could shed some new light on the problem of discrete conformal equivalence. There are many unsolved problems in the area of higher genus meshes and more general circle packings. On the application and design side, a lot of aspects have not yet been investigated. One of them, concerning efficient manufacturing, is hinted at in Fig. 19.

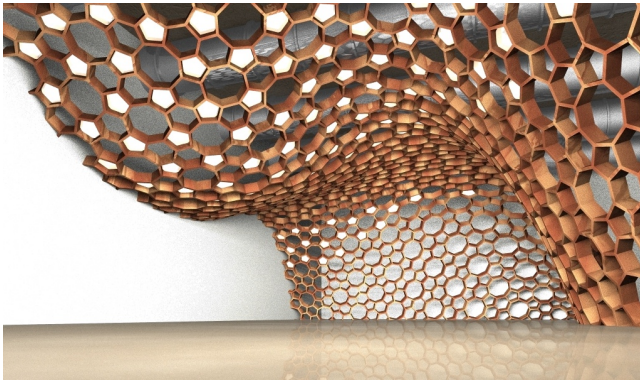


Figure 18: Derived structure with torsion-free nodes: The symmetry planes of beams nicely intersect in a common node axis whenever they meet.

Acknowledgments The authors gratefully acknowledge the support of the Austrian research promotion agency (FFG) under grant No. 813391, and the Austrian Science Fund (FWF) under grants No. S92-06 and S92-09, which are part of the National Research Network *Industrial Geometry*. We want to thank Heinz Schmiedhofer for his help in preparing illustrations and Jacques Raynaud of RFR for his fruitful comments. Further thanks go to Waagner-Biro Stahlbau, Vienna, for allowing us to present our results using real datasets.

References

- ALLIEZ, P., COLIN DE VERDIÈRE, É., DEVILLERS, O., AND ISENBURG, M. 2005. Centroidal Voronoi diagrams for isotropic surface remeshing. *Graphical Models* 67, 204–231.
- AURENHAMMER, F. 1987. Power diagrams: Properties, algorithms and applications. *SIAM J. Comput.* 16, 1, 78–96.
- BACH, K., Ed. 1990. *Radiolaria*, vol. 33 of *Publ. Inst. Lightweight Structures*. Univ. Stuttgart. (series editor: Frei Otto).
- BOBENKO, A., AND SPRINGBORN, B. 2004. Variational principles for circle patterns and Koebe’s theorem. *Trans. Amer. Math. Soc.* 356, 659–689.
- BOBENKO, A., AND SURIS, YU. 2008. *Discrete differential geometry: Integrable Structure*. No. 98 in Graduate Studies in Math. American Math. Soc.
- BOBENKO, A., HOFFMANN, T., AND SPRINGBORN, B. A. 2006. Minimal surfaces from circle patterns: Geometry from combinatorics. *Annals Math.* 164, 231–264.
- CECIL, T. 1992. *Lie Sphere Geometry*. Springer.
- CHEN, Y., DAVIS, T. A., HAGER, W. W., AND RAJAMANICKAM, S. 2008. Algorithm 887: CHOLMOD, supernodal sparse Cholesky factorization and update/downdate. *ACM Trans. Math. Softw.* 35, 3, #22, 1–14.
- GU, X. D., AND YAU, S.-T. 2008. *Computational Conformal Geometry*. International Press.
- HE, Z. X., AND SCHRAMM, O. 1993. Fixed points, Koebe uniformization and circle packings. *Annals Math.* 137, 369–406.
- JIN, M., KIM, J., LUO, F., AND GU, X. D. 2008. Discrete surface Ricci flow. *IEEE Trans. Vis. Comput. Graph.* 14, 5, 1030–1043.

- JIN, M., ZENG, W., LUO, F., AND GU, X. D. 2009. Computing Teichmüller shape space. *IEEE Trans. Vis. Comput. Graph.* 15, 3, 504–517.
- LIU, Y., POTTMANN, H., WALLNER, J., YANG, Y.-L., AND WANG, W. 2006. Geometric modeling with conical meshes and developable surfaces. *ACM Trans. Graphics* 25, 3, 681–689. Proc. SIGGRAPH.
- LIU, Y., WANG, W., LÉVY, B., SUN, F., YAN, D.-M., LU, L., AND YANG, C. 2009. On centroidal Voronoi tessellation – energy smoothness and fast computation. *ACM Trans. Graphics*. to appear. CS Tech. Report 2008-18, Univ. Hong Kong.
- LUO, F., GU, X. D., AND DAI, J. 2008. *Variational Principles for Discrete Surfaces*. International Press.
- LUO, F. 2004. Combinatorial Yamabe flow on surfaces. *Commun. Contemp. Math* 6, 765–780.
- POTTMANN, H., ASPERL, A., HOFER, M., AND KILIAN, A. 2007. *Architectural Geometry*. Bentley Institute Press.
- POTTMANN, H., BRELL-COKCAN, S., AND WALLNER, J. 2007. Discrete surfaces for architectural design. In *Curves and Surface Design: Avignon 2006*. Nashboro Press, 213–234.
- POTTMANN, H., LIU, Y., WALLNER, J., BOBENKO, A., AND WANG, W. 2007. Geometry of multi-layer freeform structures for architecture. *ACM Trans. Graphics* 26, 3, #65, 1–11. Proc. SIGGRAPH.
- POTTMANN, H., KILIAN, A., AND HOFER, M., Eds. 2008. AAG 2008 – Advances in Architectural Geometry. Proceedings of the Conference in Vienna, September 13–16.
- SPRINGBORN, B., SCHRÖDER, P., AND PINKALL, U. 2008. Conformal equivalence of triangle meshes. *ACM Trans. Graphics* 27, 3, #77, 1–11. Proc. SIGGRAPH.
- SPUYBROEK, L. 2004. *NOX: Machining Architecture*. Thames & Hudson.
- STEPHENSON, K. 2005. *Introduction to Circle Packing*. Cambridge Univ. Press.
- TOLEDO, S., 2003. TAUCS, a library of sparse linear solvers. C library, <http://www.tau.ac.il/~stoledo/taucs/>.
- YANG, Y.-L., GUO, R., LUO, F., HU, S.-M., AND GU, X. D. 2009. Generalized discrete Ricci flow. *Computer Graphics Forum* 28, 7. to appear, Proc. Pacific Graphics.

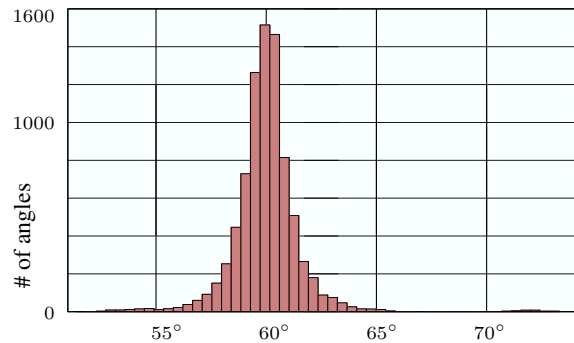


Figure 19: Histogram of interior angles of triangles of the CP mesh shown by Fig. 6a. The small standard deviation from the mean value 60° implies good packing properties of panels in all derived structures and could be exploited for the possible standardization of nodes.